

Wave-tide interaction modulates nearshore wave height

Lewis, Matt J.; Palmer, Tamsin; Hashemi, Resa; Robins, Peter; Saulter, Andrew; Brown, Jenny; Lewis, Huw; Neill, Simon

Ocean Dynamics

DOI:

[10.1007/s10236-018-01245-z](https://doi.org/10.1007/s10236-018-01245-z)

Published: 01/03/2019

Publisher's PDF, also known as Version of record

[Cyswllt i'r cyhoeddiad / Link to publication](#)

Dyfyniad o'r fersiwn a gyhoeddwyd / Citation for published version (APA):

Lewis, M. J., Palmer, T., Hashemi, R., Robins, P., Saulter, A., Brown, J., Lewis, H., & Neill, S. (2019). Wave-tide interaction modulates nearshore wave height. *Ocean Dynamics*, 69(3), 367-384. <https://doi.org/10.1007/s10236-018-01245-z>

Hawliau Cyffredinol / General rights

Copyright and moral rights for the publications made accessible in the public portal are retained by the authors and/or other copyright owners and it is a condition of accessing publications that users recognise and abide by the legal requirements associated with these rights.

- Users may download and print one copy of any publication from the public portal for the purpose of private study or research.
- You may not further distribute the material or use it for any profit-making activity or commercial gain
- You may freely distribute the URL identifying the publication in the public portal ?

Take down policy

If you believe that this document breaches copyright please contact us providing details, and we will remove access to the work immediately and investigate your claim.



Wave-tide interaction modulates nearshore wave height

Matt J. Lewis¹ · Tamsin Palmer² · Resa Hashemi³ · Peter Robins¹ · Andrew Saulter² · Jenny Brown⁴ · Huw Lewis² · Simon Neill¹

Received: 3 July 2018 / Accepted: 26 December 2018
© The Author(s) 2019

Abstract

The combined hazard of large waves occurring at an extreme high water could increase the risk of coastal flooding. Wave-tide interaction processes are known to modulate the wave climate in regions of strong tidal dynamics, yet this process is typically omitted in flood risk assessments. Here, we investigate the role of tidal dynamics in the nearshore wave climate (i.e. water depths > 10 m), with the hypothesis that larger waves occur during high water, when the risk of flooding is greater, because tidal dynamics alter the wave climate propagating into the coast. A dynamically coupled wave-tide model “COAWST” was applied to the Irish Sea for a 2-month period (January–February 2014). High water wave heights were simulated to be 20% larger in some regions, compared with an uncoupled approach, with clear implications for coastal hazards. Three model spatial resolutions were applied (1/60°, 1/120°, 1/240°), and, although all models displayed similar validation statistics, differences in the simulated tidal modulation of wave height were found (up to a 10% difference in high water wave height); therefore, sub-kilometre-scale model resolution is necessary to capture tidal flow variability and wave-tide interactions around the coast. Additionally, the effects of predicted mean sea-level rise were investigated (0.44–2.00 m to reflect likely and extreme sea-level rise by the end of the twenty-first century), showing a 5% increase in high water wave height in some areas. Therefore, some regions may experience a future increase in the combined hazard of large waves occurring at an extreme high water.

Keywords Flood risk · Combination hazard · Waves · Wave-tide interaction · Modelling

1 Introduction

Coastal flooding from an extreme sea level event is driven by the combination of storm tides (tides and surges) and waves (Lewis et al. 2013, 2011). This extreme water-level condition can overtop or breach a coastal defence, resulting in inundation (e.g. Brown et al. 2010). It is therefore crucial to understand how these flooding processes interact, and combine, to increase the hazard—especially in the coming century as

coastal flood risk is expected to increase (e.g. Leonard et al. 2014; Arns et al. 2017).

Waves contribute directly to an extreme water-level through wave breaking and run-up process; for example, wave set-up at a local level has been calculated to further increase the water levels by up to 0.5–1.0 m in Liverpool Bay (Brown 2010). Wave overtopping of a coastal defence can lead to inundation (Wolf 2008; Phillips et al. 2017), but can also cause erosion (Wolf 2009), enabling waves to propagate further inshore and thus increasing flood risk: through increased wave overtopping and the possibility of flood defence failure (van der Meer et al. 2009). Flood risk is also influenced by the pre-storm beach morphology and defence fragility, both of which may be changed during a succession of events or seasonal variability in beach level. Therefore, the combination hazard of waves and extreme high waters is essential to resolve within flood risk understanding, especially as wave and tides are known to interact (Wolf 2009).

In order to operationally determine the extreme water-level hazard for a given scenario, hydrodynamic models at a national scale are often used to provide boundary conditions to local storm impact models, which are used to simulate the consequent wave run-up, wave overtopping, or overwash (Souza

This article is part of the Topical Collection on the *15th International Workshop on Wave Hindcasting and Forecasting in Liverpool, UK, September 10–15, 2017*

Responsible Editor: Diana Greenslade

✉ Matt J. Lewis
m.j.lewis@bangor.ac.uk

¹ School of Ocean Sciences, Bangor University, Bangor, UK

² Met Office, Exeter, UK

³ University of Rhode Island, South Kingstown, RI, USA

⁴ National Oceanography Centre, Liverpool, UK

et al. 2013). Phase averaged spectral wave models and shallow-water equation models are typically used at the basin-scale. Higher fidelity (wave resolving and non-hydrostatic hydrodynamic) models are typically used within the surf zone to determine the hazard drivers impacting coastal defence schemes, with wave overtopping and inundation models used beyond the flood defence (e.g. Prime et al. 2015).

In many recently developed systems, unstructured modelling techniques have been applied in order to resolve many of the physical processes within an extreme flooding event from the basin-scale to local-scale and inundation/damage extent (e.g. Westerink et al. 2008; Bunya et al. 2010; Dietrich et al. 2011; Roland et al. 2012; Hope et al. 2013). However, compound flood risk and wave-tide interaction effects on coastal flooding in particular have often been understudied. For example, although large-scale numerical models simulate wave and storm tide (tide plus storm surge) processes, these are often run independently in operational forecast systems. In coastal flood systems design, there is a tendency to concentrate on the first order effect of depth variations on waves at the local scale, whilst neglecting potentially important broader scale effects that may be had on the wave field as a result of interactions between waves and current offshore (e.g. Ardhuin et al. 2017).

The analytical solution to the effect of currents on waves (in the absence of wave breaking processes) is given by Phillips (1977): $\frac{A}{A_0} = \frac{c_0}{\sqrt{c(c+2U)}}$; where wave amplitude (A) and phase speed (C) are modified (to A_0 and c_0) due to an ambient current (U). The resultant change in water depth due to tidal elevation also changes wave refraction, which can modulate the nearshore wave climate (Hashemi et al. 2016). Therefore, in regions of strong tidal dynamics, wave-tide interaction is likely to significantly affect the far-field wave climate propagating towards the coast and thus coastal hazards.

The interaction of tides and other flood risk drivers (i.e. waves) is important to understand, particularly in regions of large tidal range where flooding coincides with the high tide (Pugh 1996; Muis et al. 2016). Analysis of global tidal data (FES2012; Carrere et al. 2012) indicates that ~10% of the world's coastlines experience macro-tidal conditions (tidal range >4 m, using the four major tidal constituents of M2, S2, K1 and O1; see Neill et al. 2018). Over 600 million people are estimated to live in low-lying coastal regions (McGranahan et al. 2007; Muis et al. 2016), and, as coastal bathymetry often enhances tidal currents (Lewis et al. 2015), the contribution of wave-tide interaction to combination flood hazard (and how this may change) is essential to resolve. For example, the UK is one such region with macro-tidal conditions (including the second largest tidal range in the world), where approximately 6 million properties are exposed to some degree of flood risk (Prime et al. 2015).

The interaction between the tide and surge is well-known (e.g. Horsburgh and Wilson 2007), and is included with extreme water-level estimates using joint probability methods (e.g. applying skew surge to the harmonically predicted tide). The co-occurrence of waves and extreme water levels is also included within rigorous flood risk assessments (e.g. Prime et al. 2016); however, the modulation of offshore wave height due to wave-tide interaction processes is typically omitted in flood risk scenarios. Hence, if waves are likely to be larger towards times of high water, when flood risk is higher, wave-tide interaction needs to be included within flood risk assessment (Wolf 2009).

1.1 Wave-tide interaction

The transfer of momentum and energy from the atmosphere to the sea, via wind waves, is complex and considered to require a coupled modelling approach due to their interaction (e.g. Wolf 2009). Currents affect wave generation (i.e. apparent wind speed), enhance the total bottom friction (thus alter tidal current speed; e.g. Lewis et al. 2014) and result in wave refraction due to the Doppler shift (e.g. Hashemi et al. 2016). The propagation of waves in shallow water is also dependent on water depth (i.e. shoaling or refraction of waves), and, through wave set-up and wave radiation stresses, waves also alter water levels (see Wolf 2009; Staneva et al. 2016). Therefore, the tidal modulation of water levels and currents can also modulate the wave climate, which in turn affects water levels and currents, hence the principles of wave-tide interaction.

Much research has focused on the impact of wave-tide interaction to source (i.e. wave generation, see Rapizo et al. 2018) and sink (i.e. wave dissipation, see Rapizo et al. 2017) effects within simulated wave fields (see Fan et al. 2009a, b); for example, which leads to the reported “southern ocean bias” within AOGCM models (see Flato et al. 2013; Hemer et al. 2013). Many studies show the importance of wave-current interaction (e.g. Holthuijsen and Tolman 1991), with significant wave height (H_s) typically varying by 10 to 20% due to currents (Ardhuin et al. 2012). However, the influence of wave-tide interaction on compound flood risk in specific regions is still broadly understudied.

The strong tidal dynamics of UK waters are known to give rise to a tidal signal within wave buoy observations (Palmer et al. 2015; Hashemi et al. 2016), and has been studied with the use of dynamically coupled models in shallow macro-tidal regions, such as the Irish Sea (UK), where Brown et al. (2011) found a large effect of tides on waves (~10% for wave height) in areas where currents are larger (around headlands and coastal areas). Further, the influence of the tide can change wave height and refraction (due to apparent change in wave period from Doppler shift) causes the wave climate to modulate with the period of the tide

(Hashemi et al. 2016); hence, larger wave heights could coincide with high water for some regions and increase the risk of flooding.

The European wave and storm surge climate appears to show no substantial trend, with no projected change above observed natural variability and high uncertainty (see Weisse et al. 2014). Conversely, sea-level rise, and the resultant changes to tidal dynamics (Pickering et al. 2017), appears likely (IPCC 2013). New dynamically coupled ocean modelling techniques have made it possible to investigate the interaction of coastal flooding processes (see Wolf 2009); however, uncertainty and sensitivity of modelling wave-tide interaction are unknown. Therefore, understanding the role of wave-tide interaction in coastal flood hazard, and how this may change in the future with sea-level rise, appears crucial. In this study, the influence of wave-tide interaction to compound coastal flood risk will be investigated using a coupled model, with the sensitivity of model resolution and future sea-level rise included—hence storm surge, and the interaction of tide-surge-wave interaction, are omitted in this study.

1.2 Modelling wave-tide interaction

Enhanced bottom stress, Stokes drift, wave forces (i.e. vortex force) and stresses (i.e. radiation stress) can be parameterised into tidal models to simulate the effect of waves on the tidal flow (e.g. Brown et al. 2011). Wave action density is conserved in presence of currents, so 3rd Generation spectral wave models can simulate current effects on waves by including time varying current and depth fields within their simulations; for example, Stokes drift, radiation stresses and the Doppler velocity effects on the wave spectrum also be parameterised (Brown et al. 2011). Therefore, by allowing data exchange between the tide and wave models, a dynamically coupled wave-tide modelling framework can be used to simulate wave-tide interaction.

A number of dynamically coupled wave-tide modelling frameworks have been developed in recent years, such as the Coupled Ocean-Atmosphere-Wave-Sediment Transport (COAWST) system (used in this study; see Section 2), or the POLCOMS-WAM (e.g. Brown 2010), and the UK Met Office UKEP program that couples NEMOocean (tides), WaveWatch III (waves) and Met Office Unified model (atmosphere); see Lewis et al. 2018. Yet, no consistent methodology or modelling framework is apparent—or has been applied to explore compound coastal flood risk. For example, spatial variation of tidal currents occurs at sub-kilometre scales along the coastline, especially in regions of high tidal flow around headlands (see Roland, et al. 2012; Lewis et al. 2015). Hence, spatial resolution of a coupled model to simulate wave-tide interaction therefore may be important, which has led to much unstructured coupled model development (e.g. Westerink et al. 2008; Bunya et al. 2010; Dietrich et al.

2011; Roland et al. 2012; Hope et al. 2013) and yet the necessary resolution appears still, broadly, unknown.

1.3 Potential future changes to wave-tide interaction

Coastal flood risk is predicted to increase in the future for most coastlines of the world due to mean sea-level rise (IPCC 2013). Recent predictions by the IPCC 5th assessment indicate global mean sea-level rise between 44 and 74 cm is likely by 2100 but that larger (i.e. 2 m) rises cannot be ruled out. In the UK, mean sea-level rise has been observed to broadly match the global mean sea-level rise (Woodworth et al. 2009), and therefore an increase in coastal flood risk due to these mean sea-level rise projections is likely. Mean sea-level rise is also predicted to change tidal dynamics (Pickering et al. 2017; Weisse et al. 2014; Pickering et al. 2012), increasing both tidal elevation and tidal currents for regions (where flow is driven by water-level differences). Sea-level rise amplification of coastal flood hazard, due to the water depth (i.e. frictional) changes affecting tide-surge-wave characteristics, has been recently shown by Arns et al. (2017); however, the effect of wave-tide interaction on future compound flooding risk is still understudied. We hypothesise changes to tidal dynamics may also change wave-tide interaction processes, increasing the coastal flood risk due to the combined hazard of large waves occurring at high tide for some regions.

1.4 Overarching aim

This paper will explore the role of wave-tide interaction on high water wave height (when the risk to coastal inundation is greatest), how this may change in the coming century, and explore the sensitivity of simulating this process in a coupled modelling system. The 2-month period (January to February 2014) was chosen because of the exceptional series of intense storms and huge wave conditions (both long period swell wave and shorter period storm wave conditions), which resulted in persistent flooding throughout the UK (Sibley et al. 2015; Kendon and McCarthy 2015; Huntingford et al. 2014). The Irish Sea was chosen as it is a region of large tidal range and associated tidal currents, which are known to modulate the wave climate. The wave climate of the Irish Sea is also known to spatially vary; swell dominated wave climate in southern and central Irish Sea that is exposed to Atlantic waves, with fetch-limited wave climate in northern Irish Sea.

The coupled modelling approach used in this study is described in Section 2, and three results are explored: (1) the mean effect to wave height at the time of high water between a coupled and uncoupled model; (2) the effect of spatial model resolution on wave height at the time of high water; (3) the effect of sea-level rise on coupled model simulated wave height at the time of high water.

2 Methodology

The COAWST modelling system is used here to simulate the dynamic interaction between waves and tides. The COAWST model has been successfully implemented in a number of studies of the Irish Sea region (e.g. Lewis et al. 2014), and is similar to previous studies of wave-tide interaction in the Irish Sea (Brown et al. 2010; Brown et al. 2011). To determine the effect of tidal dynamics on wave propagation and generation in the Irish Sea, the wave model was run both coupled and uncoupled. The difference in simulated wave height between the coupled and uncoupled model runs was used to determine the modulation of wave height due to the tide.

The COAWST system comprises of the ocean model Regional Ocean Modelling System (ROMS), the atmospheric model WRF and the Simulating Waves Nearshore (SWAN) wave model—which is described in Warner et al. (2008a, b) and Hashemi et al. (2015). Data exchange between these modules is conducted with the Model Coupling Toolkit (Warner et al. 2008b; Warner et al. 2010). Two-way processes coupling in COAWST includes wave refraction by currents, bottom friction due to combined currents and waves, enhanced wind drag due to waves, and 3D interactions of Stokes drift, radiation stress and Doppler velocity. Therefore, wave-tide interaction can be simulated to investigate the effect of the tide on the modulation of wave height.

Three model spatial resolutions were used to investigate this effect to our results; defined here as Coarse ($1/60^\circ$), Medium ($1/120^\circ$), Fine ($1/240^\circ$), which is consistent with previous studies (Lewis et al. 2015). The “Medium grid” was used to investigate potential changes from mean sea-level rise and the overall effect of tides on waves. Two months were simulated (January–February 2014) as both extreme (wave heights and wave periods in excess of 8 m and 11 s, respectively) and quiescent conditions occurred. Model computed wave and tide results from this 2-month period were output at 1 h frequency, with data exchange between the wave and tide model every 600 s (an unpublished sensitivity test showed no significant difference to results with changes to data exchange below this frequency).

2.1 SWAN wave model

Surface waves were modelled using the SWAN third-generation spectral wave model (Booij et al. 1999). The SWAN formulation is based on the evolution of the wave action density (N) in space and time, and can be expressed as

$$\frac{DN}{Dt} = \frac{\partial N}{\partial t} + \nabla_1 \cdot [(c_g + u)N] + \frac{\partial(c_\theta N)}{\partial \theta} + \frac{\partial(c_\sigma N)}{\partial \sigma} = \frac{S}{\sigma};$$

where $\nabla_1 = \left(\frac{\partial}{\partial x}, \frac{\partial}{\partial y} \right)$ is the horizontal gradient operator; $u = (\bar{u}, \bar{v})$ represents the depth averaged current velocities with $c_\sigma = \frac{\partial \sigma}{\partial t}$ and $c_\theta = \frac{\partial \theta}{\partial t}$ as propagation velocities in spectral space. S represents the source/sink term which represents all physical processes that generate (e.g. wind), dissipate (e.g. white capping, bottom friction and depth-induced wave breaking) or redistribute wave energy (wave–wave interactions).

The group velocity is defined as $c_g = \frac{\partial \sigma}{\partial k} = \frac{1}{2} \left(1 + \frac{2kd}{\sinh(2kd)} \right) \frac{\sigma}{k} k$; where $k = (kx, ky)$ is the wave number, and is related to the water depth (d) and wave frequency through the dispersion relation $\sigma^2 = gk \tanh(kd)$. The absolute angular frequency of waves (ω) which is observed in a stationary frame like a wave buoy or a wave energy device is modified by the Doppler shift $\omega = \sigma + k \cdot u$.

Action density is conserved in the SWAN formulation (as opposed to the energy density); therefore, the effect of currents on waves can be simulated as $N(x, t; \sigma, \theta) = E/\sigma$; where σ is the relative angular wave frequency which is not affected by the Doppler shift. This enables the effect of tides on waves to be simulated in SWAN through the modulation of water depth (d) and currents (u) due to tides, as input files from model coupling (see Hashemi et al. 2015; Lewis et al. 2014).

To simulate far-field generated waves propagating into the Irish Sea, a SWAN model of the northwest European shelf sea was used, which has already been extensively validated (e.g. Neill and Hashemi 2013) and applied in previous studies (e.g. Lewis et al. 2014; Lewis et al. 2017). The entire North Atlantic was simulated at a grid resolution of $1/6^\circ$, extending from 60°W to 15°E and from 40°N to 70°N . A one-way nest (with 2D wave spectra) to the higher resolution SWAN model of the Irish Sea was then applied, at the spatial resolutions of the ROMS computational grid (see next section).

Wind data from the ECMWF-ERA-Interim reanalysis product was used (see Dee et al. 2011) to force the wave model at 3-hourly intervals, with the same configuration as Neill et al. (2014): 0.75° regular grid resolution with improved horizontal resolution (~ 80 km) and 4D-Var (data assimilation). The wave energy spectrum for each grid cell was discretised into 40 frequency bins, with a directional resolution of 8° (45 direction bins for a full circle), and frequency resolved between of 0.04 and 1 Hz (25 to 1 s period waves); see Neill and Hashemi (2013).

2.2 ROMS hydrodynamic model

The ROMS is used to simulate tidal dynamics in the Irish Sea. The ROMS modelling system uses a finite-difference approximation of the 3D Reynolds-Averaged Navier-Stokes (RANS) equations, with hydrostatic and Boussinesq assumptions, with a horizontal curvilinear Arakawa C grid and terrain-following

vertical coordinate system (the sigma coordinate system) of 10 depth layers evenly spaced throughout the water column (see Lewis et al. 2015). This ROMS model has been successfully applied to previous Irish Sea tidal modelling studies (Lewis et al. 2015, 2017). Further details of the ROMS model, including the discretised full equations and model verification details, are found in a number of publications (e.g. Shchepetkin and McWilliams 2005; Haidvogel et al. 2008), and so are not described further here (see also www.myroms.org).

Digitised Admiralty data (at 200 m resolution; <http://digimap.edina.ac.uk>) was interpolated to the ROMS computational grid using a nearest neighbour approach, and corrected to mean sea-level. The domain and the bathymetry of the Irish Sea tide model are shown in Fig. 1. The geographic scale of inter-tidal regions is relatively small in relation to model resolution and extent (Lewis et al. 2015); therefore, a minimum water depth of 10 m was applied to the bathymetry data (i.e. no wetting and drying in the model), as has been previously applied to this region (e.g. Lewis et al. 2015). The open boundary of the tidal model was forced with ten tidal constituents (M2, S2, N2, K2, K1, O1, P1, Q1, Mf and Mm) from the Finite Element Solution and data assimilated global tide product (FES2012) by Carrere et al. (2012), which has shown to be accurate in this region (Lewis et al. 2015).

A constant drag coefficient (C_D) of 0.003 was assumed within the quadratic friction model parameterisation, consistent with previous studies (e.g. Lewis et al. 2014). The

interaction between waves and bed shear stress is parameterised using the SSW-BBL option in COAWST (Warner et al. 2010). In the SSW-BBL routine, the artificial bed roughness (Z_0) from wave-current interaction is based on median sediment grain size (D_{50}) of 3 mm—consistent with previous studies (e.g. Lewis et al. 2014).

The turbulence closure Generic Length Scale (GLS) model was tuned to the κ - ϵ turbulence model, including wave breaking and wave effects on current (WEC) vortex-force parameterisation (Kumar et al. 2012). Here, we use the WEC_MELLOR (Warner et al. 2010) parameterisation of radiation stress terms for waves on currents—as previously applied in the Irish Sea (Lewis et al. 2014). Therefore, conservative and non-conservative wave force effects on the simulated mean flow-field of ROMS are included within the COAWST model.

2.3 Model validation

The COAWST Irish Sea model was validated for both tides and waves (Table 1) and the location of validation data shown in Fig. 1. Eleven tide gauges (diamonds in Fig. 1) were used to validate tidal elevation, and example time-series are shown in Fig. 2. To validate the model for tidal currents, 140 sites were used (9 sites of depth averaged currents and 131 depth specific M2 tidal current sites) using data, quality controlled and processed into principle semi-diurnal lunar constituent, M2, tidal current data by the British Oceanographic Data Centre (www.bodc.ac.uk). Validation showed accurate simulation of tidal dynamics (~ 5 and 10% Normalised Root Mean Squared Error for M2 elevation and currents, respectively, and an overall R^2 value of 99%). There were no major differences in validation statistics (i.e. Normalised Root Mean Squared Error or Rsq skill) between model spatial resolutions; see Table 1.

The ROMS, sigma coordinate, 3D current fields were interpolated to validation data using a nearest neighbour approach. All tidal current validation stations were in water depths greater than 10 m. Further details of this data can be found in Lewis et al. (2015) and only briefly described here: Water depth of the current measurements varied between 143 and 3 m (mean of 58 m), which gave a wide range of 3D current validation data between the near seabed (max sensor depth at $\sim 99\%$ of water depth) to near surface (minimum sensor depth $\sim 4\%$ of water depth) and mid water column (mean sensor height at $\sim 43\%$ of water depth); as well as a wide range of current speeds (major axis of the principle semi-diurnal lunar constituent (M2) ranged between 0.03 and 1.10 m/s, with an average of 0.54 m/s).

To spatially and temporally validate the accuracy of the simulated wave climate, three wave buoys and eight satellite tracks were used (see Fig. 1). A 56-day record (3 January 2014 to 28 February 2014) from the Met Office “Aberporth” (Ab)

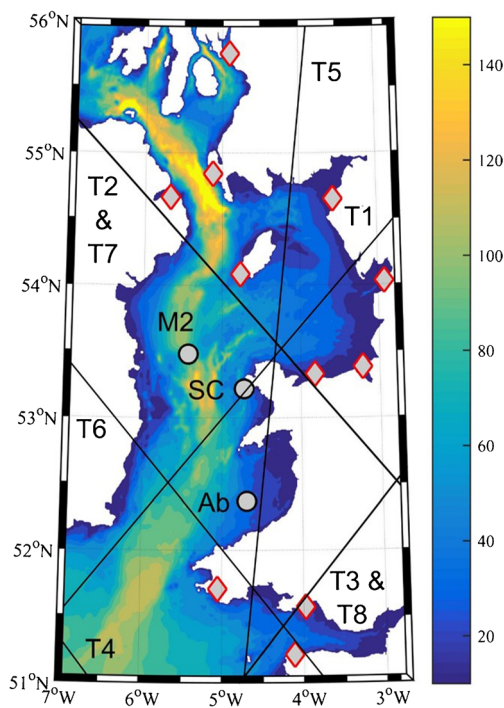


Fig. 1 Bathymetry and model domain (coloured), with locations of validation data: tide gauge stations are shown in diamonds, three wave buoys (M2, Ab, SC) and the eight satellite tracks (T1 to T8) described further in Fig. 4

Table 1 Model validation for three spatial resolutions using Root Mean Squared Error (RMSE) with (Normalised-RMSE in brackets as %). Data from 11 tide gauges (amplitude (amp) and phase (pha) of M2 and S2 tidal constituents), 9 depth-averaged M2 tidal ellipse data (major axis (Cmax), minor axis (Cmin), Inclination (Inc) and phase), 131 M2 tidal current observations at specific depths (U and V amplitude and phase), wave height (Hs) and period (T) for three wave buoy records and eight satellite tracks

		Coarse (1/60°) RMSE (NRMSE)	Medium (1/120°) RMSE (NRMSE)	Fine (1/240°) RMSE (NRMSE)
Tidal elevation	M2 amp	0.13 m (5%)	0.12 m (5%)	0.11 m (4%)
	M2 pha	6°	6°	4°
	S2 amp	0.08 m (9%)	0.08 m (9%)	0.08 m (9%)
	S2 pha	14°	14°	9°
Depth-mean M2 tidal ellipse	Cmax	0.08 m/s (11%)	0.07 m/s (10%)	0.07 m/s (10%)
	Cmin	0.02 m/s (8%)	0.02 m/s (8%)	0.02 m/s (8%)
	Inc	6°	5°	5°
	Pha	8°	7°	7°
M2 currents at specific depths	M2 Uamp	0.10 m/s (9%)	0.11 m/s (10%)	0.11 m/s (10%)
	M2 Upha	4°	4°	4°
	M2 Vamp	0.09 m/s (9%)	0.09 m/s (10%)	0.09 m/s (10%)
	M2 Vpha	6°	6°	6°
Wave buoys	Hs	0.47 m (9%)	0.58 m (11%)	0.50 m (10%)
	T	1.4 s (22%)	1.8 s (32%)	1.8 s (32%)
Satellite	Hs	0.50 m (34%)	0.51 m (36%)	0.50 m (34%)

wave buoy (52.37°N 4.69°W in 46 m water depth), a 7-day record (1 January 2014 to 11 January 2014) from the Met Erin “M2” station (53.48°N 5.43°W in 85 m water depth) and a 45-day record (3 October 2014 to 16 November 2014) from the Bangor University “Seacams” (SC) wave buoy (53.22°N 4.72°W in 46 m water depth) were used as the validation wave buoys. Wave height data from the eight satellite tracks were made available through the e-surge product (www.storm-surge.info/) and compared to the simulated wave height data

at nearest model cell. The location of the satellite tracks is shown in Fig. 1, and the dates listed in Table 2.

Overall, significant wave height (Hs) and mean wave period were simulated with accuracy (RMSE of ~0.5 m and < 2 s, respectively) and skill (e.g. R^2 of ~85% overall for Hs). Validation statistics were broadly similar for all three model spatial resolutions; as summarised in Table 1. Validation statistics (NRMSE and Rsq) were also broadly similar between the coupled (COAWST) and the uncoupled (SWAN-only)

Fig. 2 Time-series comparison of simulated astronomical tidal water-levels (η) at four tide gauge locations: Bangor Northern Ireland (BAN, 1), Milford Haven (MHA, 2), Newport (MPO, 3), Isle of Man (IOM, 4); with Root Mean Squared Error (RMSE) and Normalised Root Mean Squared Error (NRMSE) shown for January–February 2014

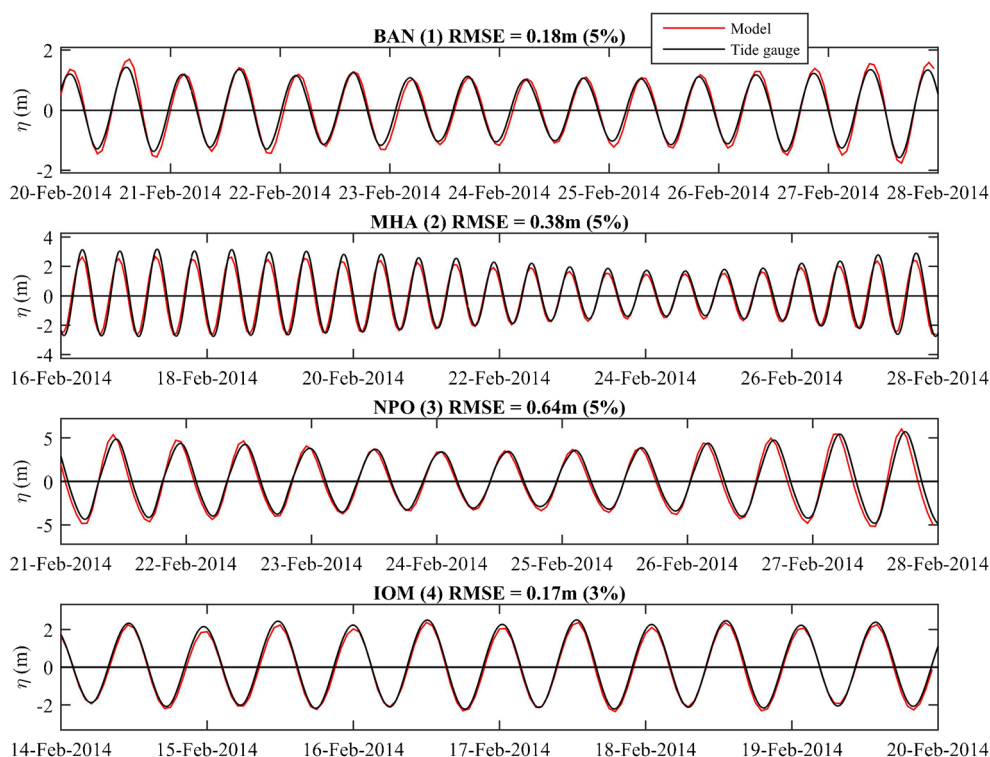


Table 2 Satellite track data for wave height spatial validation; see Figs. 1 and 4

Track (see Fig. 1 for position)	T1	T2	T3	T4	T5	T6	T7	T8
Date (dd/mm/yy) and time range	1/1/14 10:01 to 10:52	3/1/14 17:01 to 17:33	4/1/14 10:01 to 10:04	7/1/14 17:01 to 17:07	9/1/14 22:01 to 22:24	10/1/14 16:01 to 16:19	12/2/14 09:02 to 09:29	13/2/14 02:02

model at medium resolution ($1/120^\circ$ grid); an accuracy difference of 0.01 m ($< 1\%$ NRMSE) in wave height and 0.2 s ($< 2\%$ NRMSE) in wave period, with an R_{sq} difference of 2% for both these parameters: as shown in Table 3 in the appendix. The comparison of wave height simulated with the coupled and uncoupled model is shown in the more detailed analysis of wave buoys and satellite tracks in Figs. 3 and 4, respectively.

The ability of the coupled model to simulate the effect of tides on waves is further visually illustrated in Fig. 5. A short example of wave height modulating at the semi-diurnal period (~ 12.42 h), observed at the Aberporth wave buoy, is shown in Fig. 5a. A one-dimensional wave spectra comparison at the Aberporth buoy site (using FFT analysis in Matlab with a Nyquist frequency of 7200 s) found the coupled model recreates the observed 12.42 h modulation of wave height in the 2-month record (January–February 2014), whilst the wave-only uncoupled model does not, as shown in Fig. 5b. We therefore have confidence in the accuracy of the wave-tide coupled

(COAWST) Irish Sea model to simulate wave-tide interactions effects (see also Table 1).

3 Results

The percentage difference between simulated hourly wave fields of the coupled and uncoupled models was calculated to determine the modulation of wave height due to the tidal dynamics over the 2-month simulation (January–February 2014); an example of which is shown in Fig. 6. The mean percentage difference in high water wave height (δH_{sHW}) was calculated to indicate the effect of tides on waves for the period of peak flood risk. The percentage difference was used so our result is applicable with the magnitude of extreme event, as initial analysis showed the percentage mean difference a consistent value to use irrespective of the magnitude of wave height. The mean effect of the tide on high water wave height (δH_{sHW}) is shown in Fig. 7 (coupled–uncoupled high

Fig. 3 Wave height time-series from three wave buoy records compared to uncoupled (“swan”) and coupled (“COAWST”) simulated wave height (for $1/120^\circ$ resolution models)

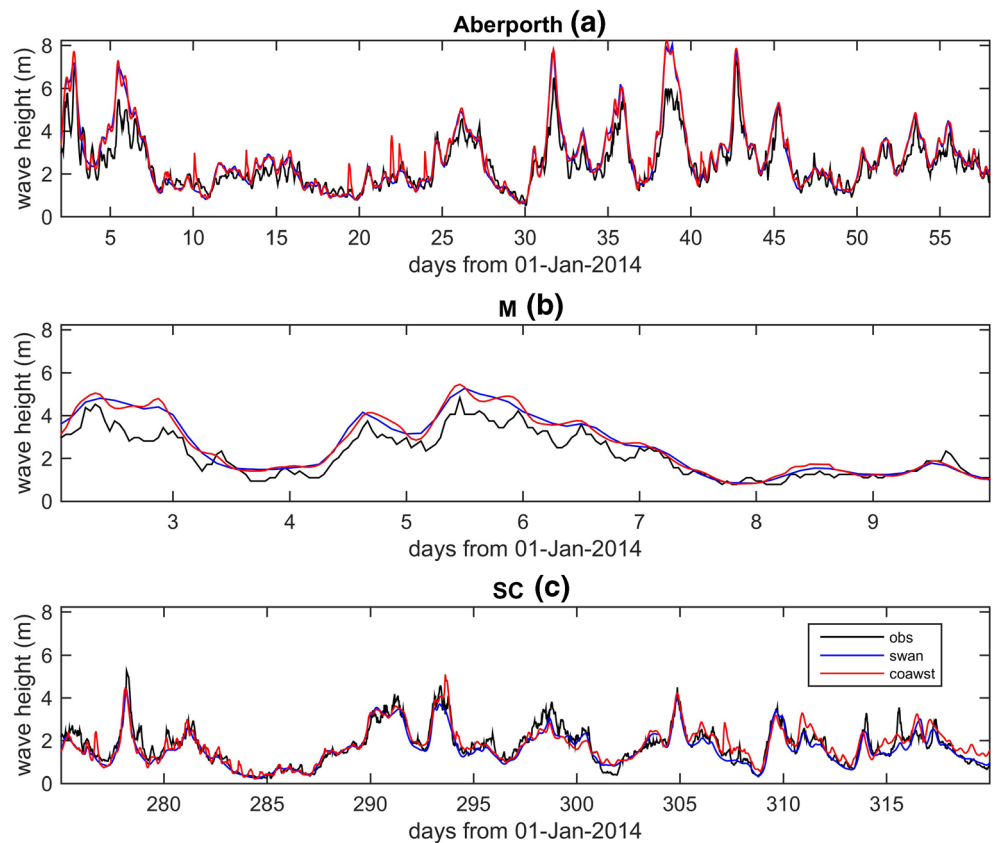
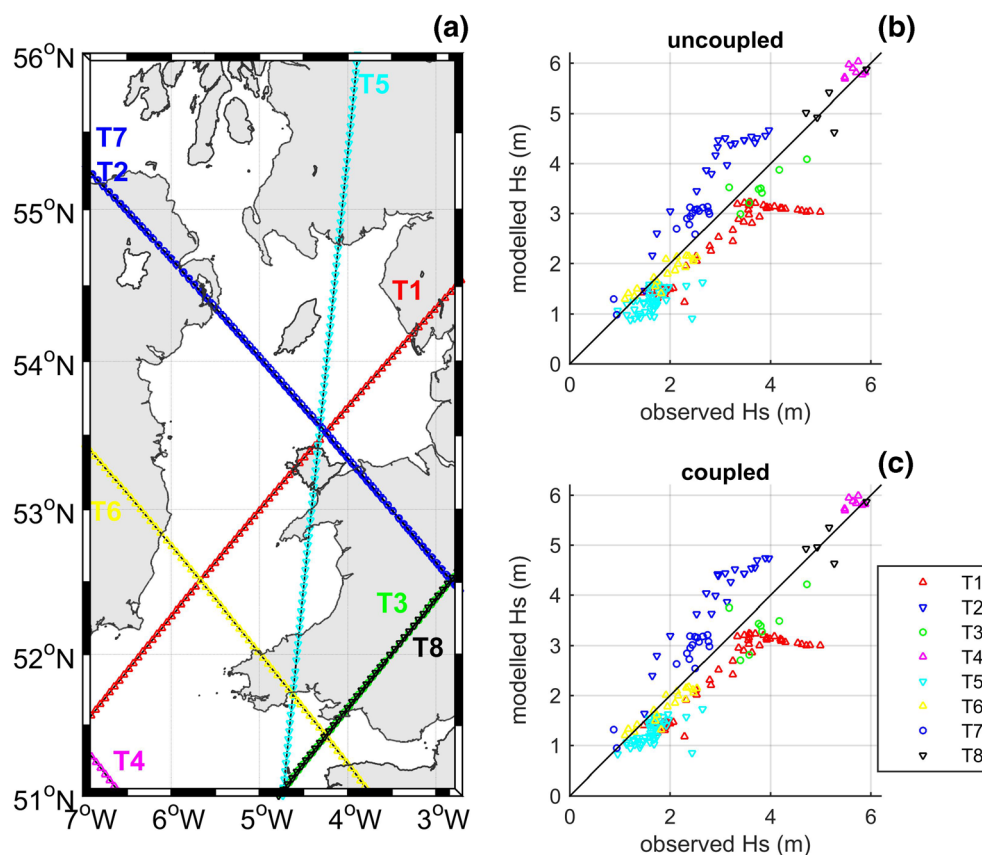


Fig. 4 Eight satellite tracks used for spatial validation of wave height (a) for the uncoupled, swan-only model (b) and the dynamically coupled wave-tide COAWST model (c) at 1/120° resolution



water significant wave height), and reveals spatial variability throughout the Irish Sea. A large effect of the tide on high water wave height (δH_{sHW}) was found around features where tidal currents are accelerated, such as the headlands along the Welsh coast (Pembrokeshire in the south and the Llyn in the

north). Furthermore, the refraction of waves around the large-scale headland features (i.e. North and South Wales), and the modulation of this refraction due to Doppler shift, results in the modulation of the wave climate with the period of the tide for bay features behind these headlands (e.g. Cardigan Bay) and large areas of the Irish Sea as waves propagate away from these regions of high tidal flow (Fig. 7).

3.1 Effect of tides on high water wave height

The effect of tidal dynamics is shown in Fig. 8, where mean changes to the high water wave height (δH_{sHW}) are clustered in regions of large tidal range and strong associated currents. Waves predominantly propagate from the Atlantic into the Irish Sea during this winter period (January–February 2014), and the effect of the tide altering wave refraction can be seen in Fig. 7, propagating from Pembrokeshire (the southern headland of Wales) into Cardigan Bay (the large bay between 52°N and 53°N) and around Anglesey into Liverpool Bay (between 53°N and 54°N).

The resultant tidal effect on wave propagation is that high water wave heights were found to be larger by up to 20%; for example in large regions of the Welsh coastline (Cardigan Bay the large bay between 52°N and 53°N)—and up to 40% off-shore (see Fig. 8). However, wave height was not larger at high tide throughout the Irish Sea, and instead an increased

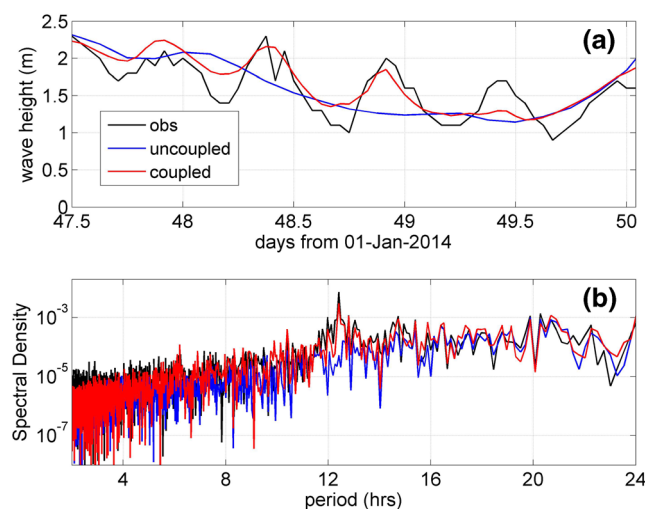


Fig. 5 A comparison of wave height (Hs) at the Aberporth Buoy (obs) to demonstrate model skill in simulating the effect of tides on waves: short time-series example (a) and 1-D wave spectra of wave height (Hs) for January–February 2014 (spectral density in m^2/s), with frequency converted to hours to show a clear modulation of Hs in both observed and coupled model data at the period of tide (12.42 h)

Fig. 6 Example of the methodology used to determine influence of tidal dynamics on high water wave height at Aberporth (52.37°N and 4.69°W). Coupled and uncoupled simulated wave height (**a**), relative to the tidal elevation (**b**), are subtracted from one another (δH_s , in panel **c**), with difference at high water (black dots) identified

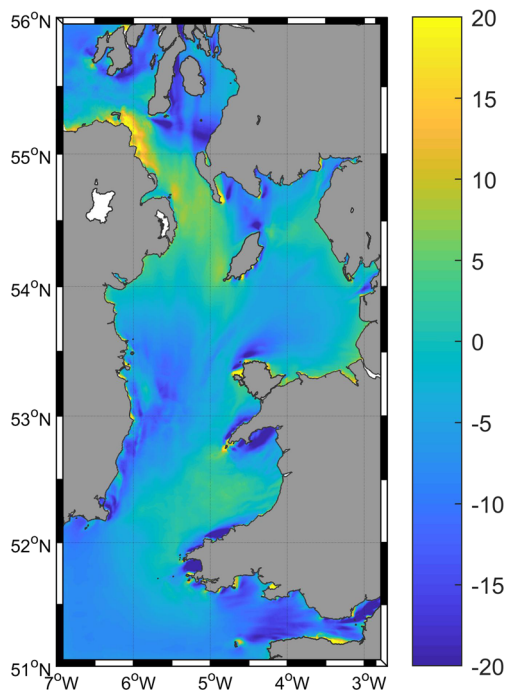
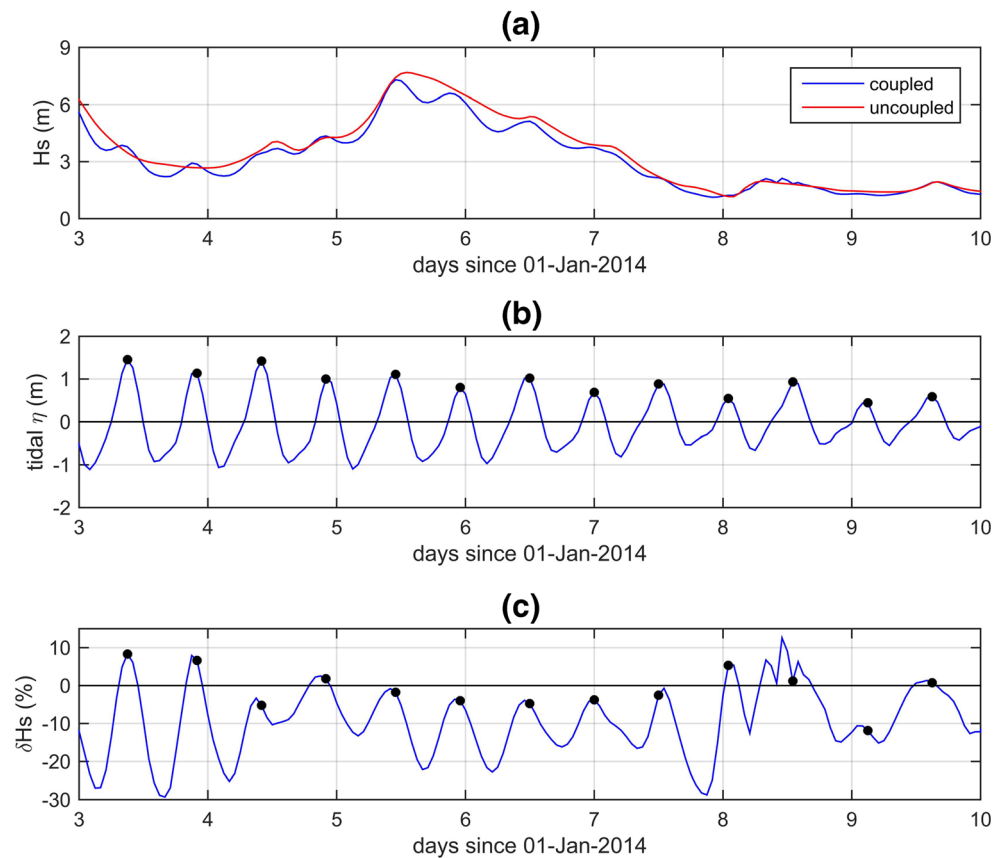


Fig. 7 The 2-month mean difference in high water wave height between coupled and uncoupled models (%); representing contribution of tidal dynamics to wave height during time of peak flood risk

wave height near low water was simulated in some regions (see Figs. 7 and 9)—likely due to localised tidal modulation of water depth or current induced refraction, which may not directly affect flood risk, but may impact nearshore erosion and sediment transport pathways. Further, the pattern of relative timing of peak wave height within a tidal cycle (i.e. average time of peak wave height due to wave-tide interaction processes), shown in Fig. 9b, is consistent with the modulation of wave refraction due to tidal current-induced Doppler shift in wave period (i.e. longer period waves on ebbing tide result in greater refraction around headlands and coupled modelled wave heights to peak on the ebb tide towards low water: see Fig. 9b's blue regions in lee of headlands from dominant Atlantic, NE propagating, wave climate).

3.2 Effect of model resolution

The effect of model spatial resolution can be seen in Fig. 10, with finer-scale features of wave height changes at high tide being resolved with higher resolution, as well as an increase (up to 5%) in the effect of tidal modulation of wave height. Changes to tidal dynamics between the three spatial resolutions as shown in Fig. 11 as changes to the peak spring tide—

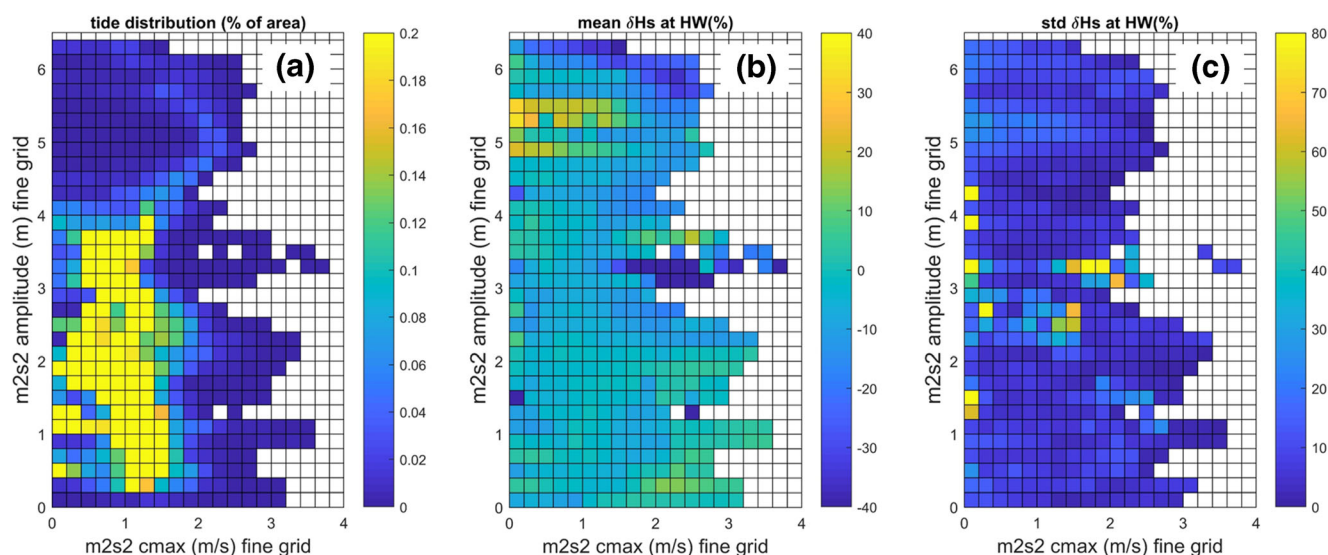


Fig. 8 Tidal influence of simulated high water wave height (δH_s at HW) discretised into distribution of the Irish Sea tidal dynamics; shown as percent of total Irish Sea area when grouped (in 0.2 m/s or m “bins”) into mean spring peak current and elevation (m2 and s2 amplitude) in

panel **a**, and used to group the corresponding tidal influence to high water wave height: mean difference (as %) of high water wave height between coupled and uncoupled models (**b**) and associated standard deviation (**c**)

so to include changes to both the M2 and S2 tidal harmonics, which dominate tides in this region.

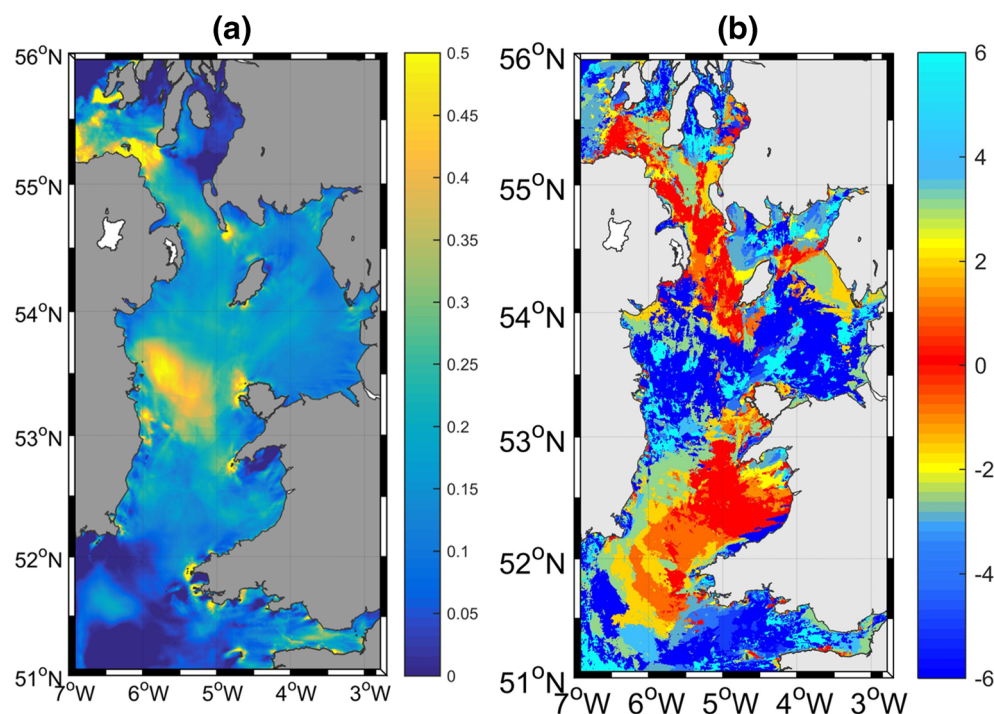
Analysis of difference in simulated tidal dynamics between the three model resolutions revealed accelerated flow around bathymetric features (e.g. headlands) was captured with a higher resolution model, and a slight change in the partial amphidromic point of Ireland ($\sim 52^\circ\text{N}$) which effects tidal dynamics throughout the Irish Sea (Cardigan Bay and the near-resonant Liverpool bay); as shown in Fig. 11. Therefore, wave-tide interaction was found to be sensitive to model spatial

resolution due to the effect of tidal current changes around bathymetric features and small changes in tidal model accuracy (as all three model resolutions validated well; see Table 1).

3.3 Effect of sea-level rise

To further explore the sensitivity of tidal dynamics on wave-tide interaction and potential future changes, three mean sea-level scenarios were simulated; 0.44, 0.74 and 2.00 m. These three mean sea-level rise scenarios correspond to the latest

Fig. 9 Effect of tidal dynamics on wave height: **a** the difference in wave height (δH_s) (between coupled and uncoupled model) for averaged for the entire 2-month record (January–February 2014) and **b** the relative timing of this tidally induced larger wave height compared to local high water (mean relative time difference of peak wave height difference (δH_s) compared to time of local high water; in hours)



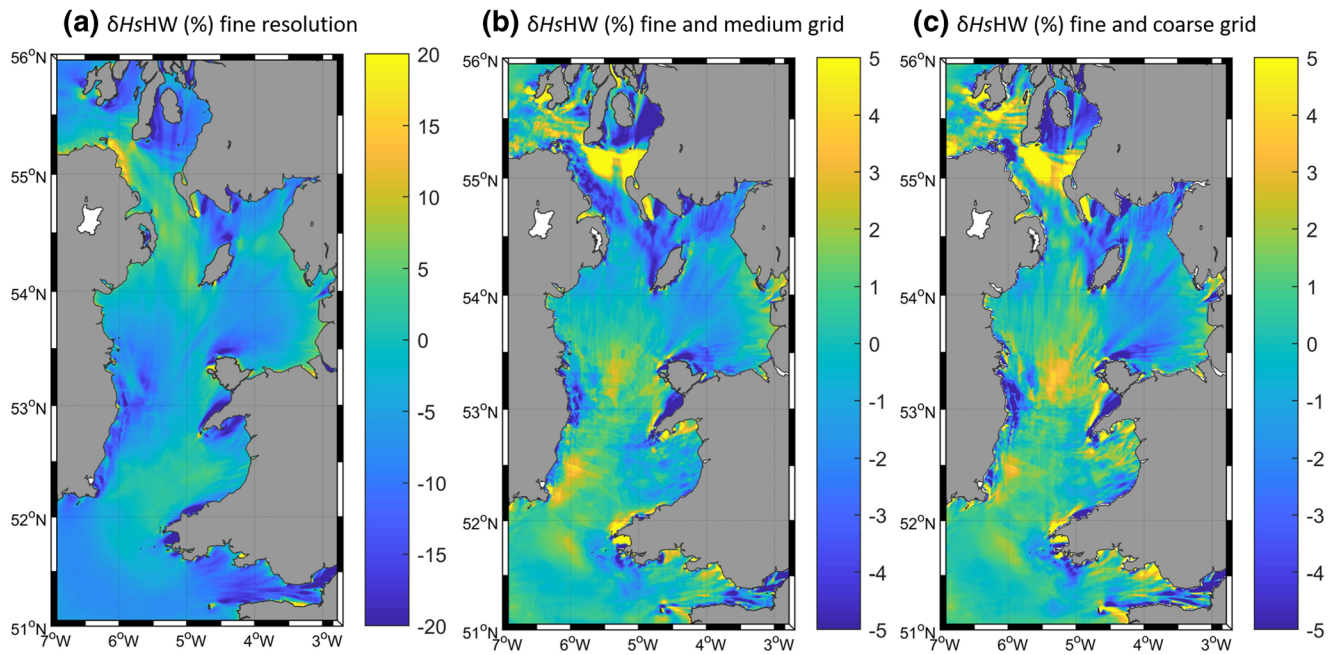


Fig. 10 Mean difference in high water wave height ($\delta HsHW$ as %, between coupled and uncoupled models for January–February 2014) for the “fine resolution” $1/240^\circ$ grid (**a**), and the relative difference (%)

compared to panel **a** for “medium resolution” $1/120^\circ$ grid (**b**) and “coarse resolution” $1/60^\circ$ grid (**c**)

IPCC 5th assessment likely global mean sea-level rise projections (and an extreme case) as the UK’s mean sea-level is rising at a similar rate to the global mean (Woodworth et al. 2009). The three mean sea-level rise scenarios were added uniformly to the bathymetry (of the ROMS medium resolution model) by “increasing” water depths by 44, 74 and 200 cm, respectively. Boundary forcing conditions (from FES2012) were assumed to be constant for future conditions and no changes to the coastline were assumed (as no wetting and drying is included). Therefore, the simulated future changes to tidal dynamics should be treated with caution, as the sensitivity of wave-tide interaction to potential changes in tidal dynamics was the objective of our work.

In all three sea-level rise scenarios, tidal dynamics were significantly altered as the increased water depth changed tidal friction; therefore, the near-resonant tidal systems to the north and south of Wales (the higher amplitude regions of Fig. 12) and Ireland partial amphidromic position were altered (the lower amplitude regions of Fig. 12), affecting tidal dynamics throughout the Irish sea. The subsequent changes to tidal current speeds due to changes in tidal friction (i.e. water depth) and near-tidal resonance are shown in Fig. 13. The influence of these potential changes to future tidal dynamics from sea-level rise to wave-tide interaction is shown in Fig. 14. The relative change of mean high water wave height was found in all sea-level rise scenarios, with an increase in high water wave height for the majority of the Welsh coastline. Therefore, although there is uncertainty (and low confidence of accuracy) in our simulated changes to future tidal dynamics, the

potential effect to coastal flood risk is clear; wave-tide interaction can lead to increased wave heights at high water for some geographic regions, and this effect may amplify in the future.

4 Discussion

The effect of wave-tide interactions on high water wave height was explored using a wave-tide coupled model, for a 2-month period (January and February in 2014) observed to be the stormiest period of weather within 20 years (Huntingford et al. 2014; Kendon and McCarthy 2015) when a number of high-energy wave events resulted in coastal flooding (Sibley et al. 2015). The simulated tidal modulation of wave height matches previous studies of the Irish Sea, where tides modulated wave heights by $\sim 10\%$ in some areas (Brown et al. 2011; Hashemi et al. 2015).

In our study, wave-tide interaction increased high water wave height by up to 20% for regions of the coastline where modulation of waves coincided with local high water (Fig. 7). As overtopping hazard increases exponentially with wave height (Pullen et al. 2007), such an increase is also likely to exponentially increase flood risk (see Stockdon et al. 2006). Therefore, for these regions of increased wave height at high water, boundary condition uncertainty needs to be propagated into flood hazard impact models, and joint probability modelling scenarios of flood risk required (e.g. Prime et al. 2016). For example, the modulation of wave height in a

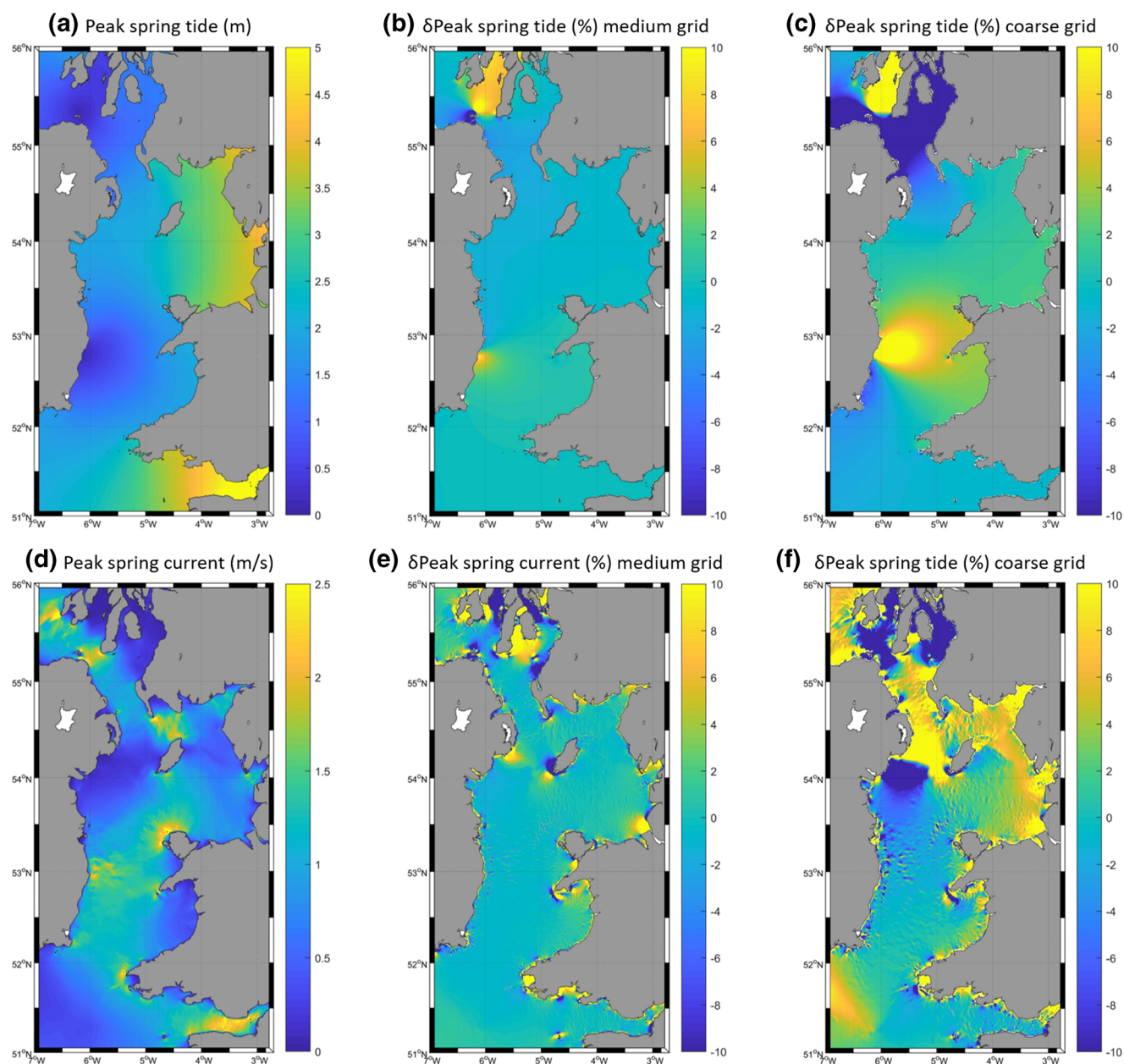


Fig. 11 Simulated differences in spring tidal dynamics (M2 and S2 harmonics) between three model resolutions; tidal amplitude of the fine resolution 1/240° grid (**a**), with the relative difference (%) compared to

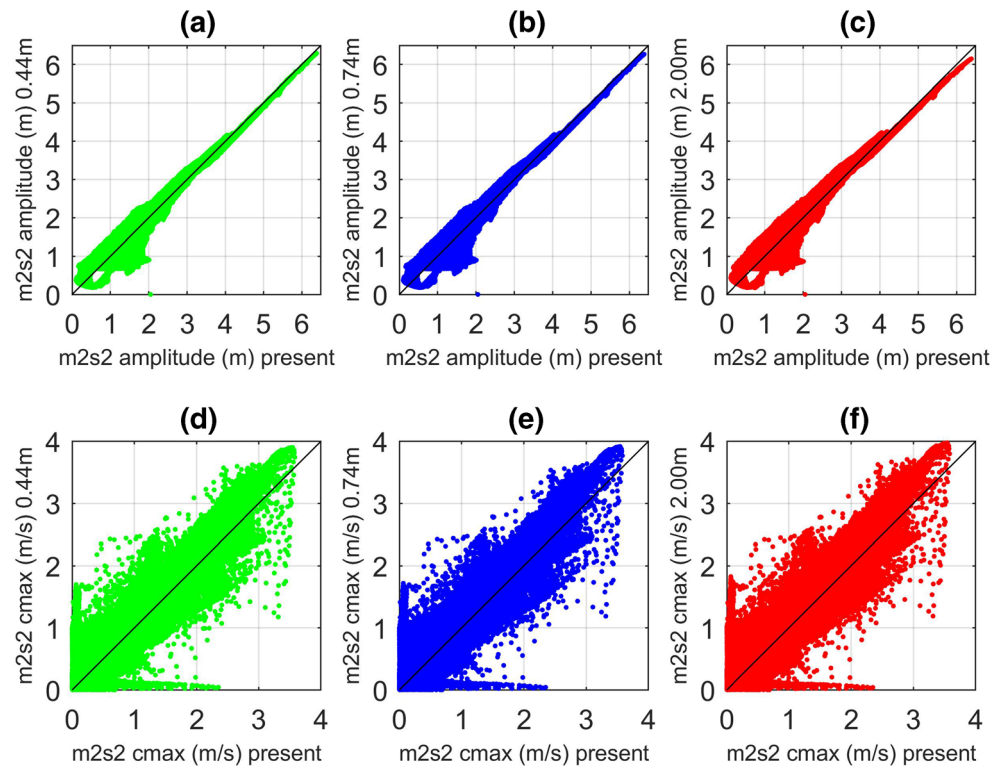
“medium” 1/120° (**b**) and “coarse” 1/60° grid (**c**). Major spring tidal ellipse component (c_{max}) of fine resolution grid (**d**), with the relative difference (%) compared to the “medium” (**e**) and “coarse” grid (**f**)

tidal signal could be propagated through overtopping models (e.g. EUROTOP; Pullen et al. 2007), and multiple flooding drivers (e.g. erosion effects and tidal variations to wave height), then cascaded through to inundation extent (e.g. within LISFLOOD modelling frameworks; see Gallien et al. 2014).

Increased wave action on coastal defences (altering coastal defence fragility and wave overtopping rates), as well as wave erosion and increased wave run-up (e.g. Wolf 2009) is likely to further increase the combined flood risk, when considering the tidal modulation of nearshore wave height shown in this study; however, the accurate assessment to the combination

hazard of coastal flooding is likely to be a complex task, requiring multiple input parameters (beach morphology, coastal defence structures, river discharge, water-level and wave climate). For example, the spatial scales of the modelling presented in this study are too coarse for drawing many if any conclusions in the nearshore portions of the domain (i.e. our study does not resolve processes in the surf zone). However, the results shown here could be propagated through higher fidelity coastal zone modelling techniques to resolve the likely impact of wave-tide interaction to coastal flood risk. One potential solution could be an unstructured modelling

Fig. 12 Future changes to the spring tidal amplitude (m2 and s2 amplitude harmonics) for present day, and the relative change when applying 0.44 m (a), 0.74 m (b) and (c) 2.00 m mean sea-level rise (MSLR) scenarios, with subsequent changes to the peak spring tidal current (cmax of the m2 and s2 harmonics) shown for the these three sea-level rise scenarios (panels d, e and f, respectively)



approach to resolve much of the surf zone processes omitted within the study (e.g. Bunya et al. 2010; Dietrich et al. 2011; Roland et al. 2012; Hope et al. 2013); however, the computational burden of simulating combined hazard events at regional-scale (i.e. multi-month morphodynamic, wave-tide coupled, fluvial and oceanic flood risk driver simulations) would be exceedingly challenging (especially at regional-scale, with multi-ensemble runs such as typical within flood forecasting).

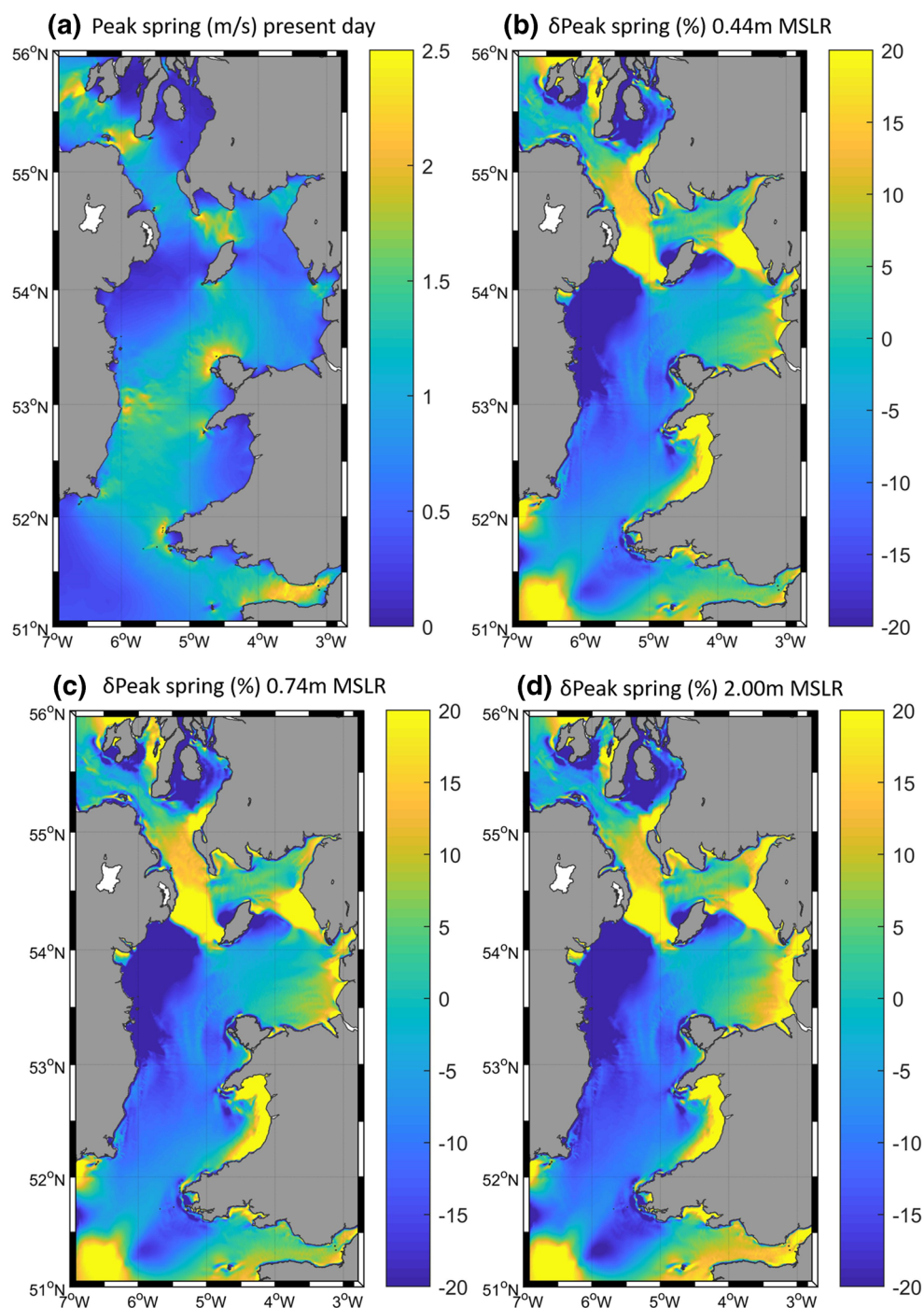
The spatial variability of wave height affected by wave-tide interaction processes (Fig. 9) indicates the process behind higher waves at high tide for some regions (Fig. 7): a large effect of the tide on wave height was found around features where tidal currents are accelerated, such as the headlands of Wales (Pembrokeshire in the south and the Llyn in the north; see Fig. 9) and as predicted by Phillips (1977). Further, the tidal current field will affect refraction of waves due to Doppler shift (such as around the large-scale headland features in North and South Wales), resulting in the modulation of wave propagation into the bay features behind these headlands (e.g. Cardigan Bay) and for large areas of the Irish Sea (waves predominantly propagate northwards from the Atlantic exposed south).

The timing of the tidal modulation to wave height (e.g. Fig. 5) coincides as an increase in wave height around high water for some regions (Fig. 7), with clear flood risk implications. However, wave height was also found to increase around low water in other regions, especially for regions of strong tidal currents, and this may result in changes to erosion

and sediment transport pathways due to enhanced bed shear stress from the combined effect of waves and currents (Hashemi et al. 2015). Future work should therefore investigate potential changes to sediment transport pathways from wave-tide interaction and likely sea-level rise. Moreover, surges will also change water depth (and currents) and river input could be very important for communities within estuaries; therefore, wave-tide-surge-river interaction could also be the focus of future work for accurate representation of extreme flood hazard conditions (e.g. Maskell et al. 2013).

Clear differences in the simulated wave height at high tide were found using three model resolutions, although the pattern was broadly similar (Fig. 10). As tidal currents are accelerated by bathymetric features, coupled wave-tide models need to include these fine-scale spatial features. Hence, model spatial resolution is important for accurate simulation of tidal current fields around complex coastlines, whilst spatial variability of tidal elevation is small (see Fig. 11). Previous studies have shown sub-kilometre-scale resolution is needed to accurately resolve tidal currents (Lewis et al. 2015), and therefore a similar resolution should be sought after in wave-tide coupled modelling at shelf scales—such as applying an unstructured grid approach (e.g. Roland et al. 2012). Furthermore, differences in the simulated tidal dynamics were clear between the three model resolutions, and yet their validation was broadly similar (Table 1). Indeed, in some regions the difference in simulated wave height between the coupled and uncoupled models was of the same order of magnitude as the validation.

Fig. 13 Future changes to peak spring tidal current (cmax of the m2 and s2 harmonics) for present day **(a)**, and the relative change (as % of panel **a**) applying 0.44 m **(b)**, 0.74 m **(c)** and 2.00 m **(d)** mean sea-level rise (MSLR) scenarios

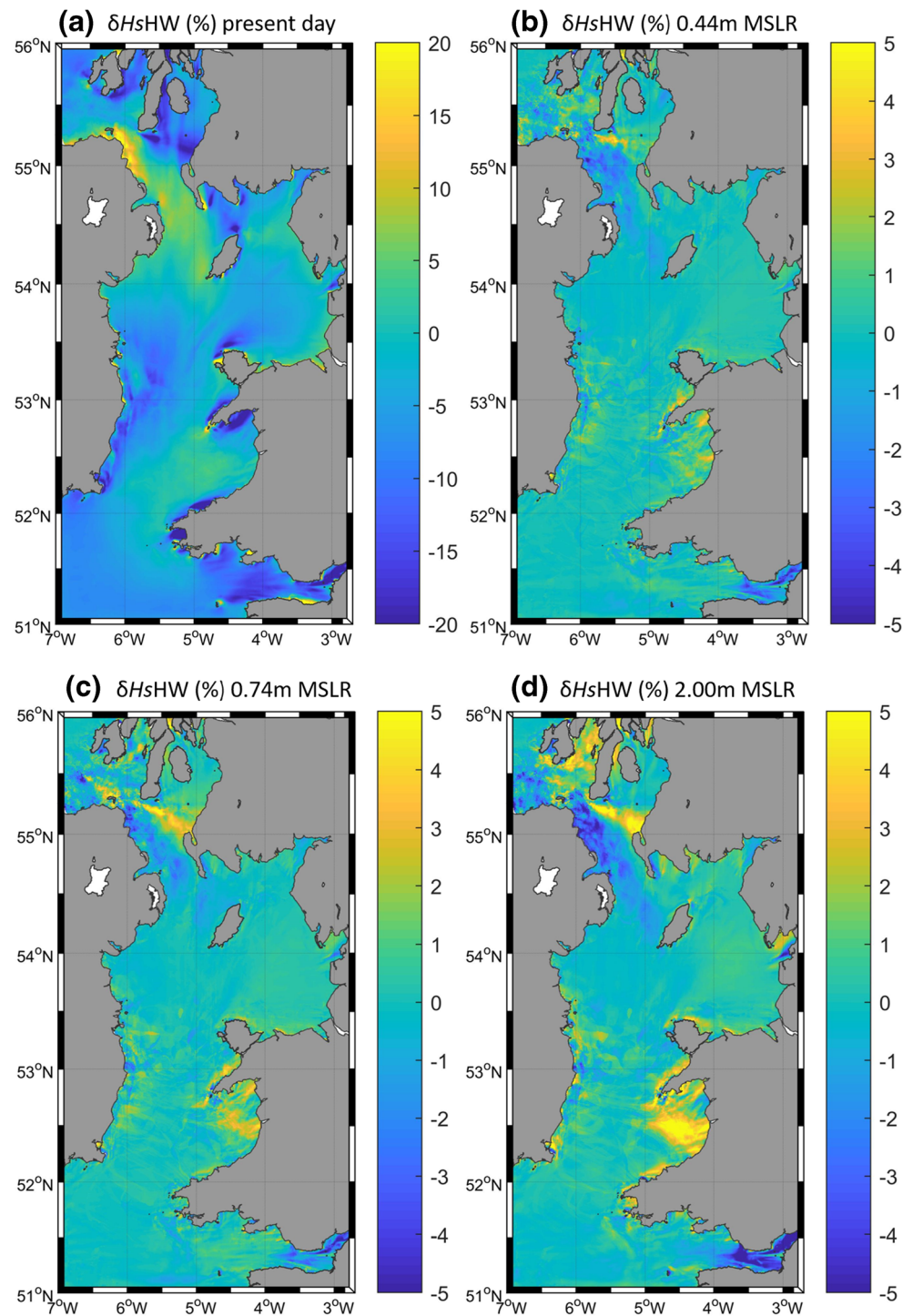


Therefore, future work should investigate improved methods of validation—beyond our visual comparison (Fig. 5) and traditional methods (e.g. nearshore wave climate observations and improved validation statistics, such as wavelet analysis; see Palmer et al. 2015).

The effect of sea-level rise was shown to increase the simulated wave-tide interaction processes for three scenarios: 0.44, 0.74 and 2.00 m mean sea-level rise. The increased water depth, and subsequent reduced tidal friction within our

model, significantly changes both tidal amplitudes (Fig. 12) and tidal currents (Fig. 13) in the Irish Sea. The enhanced tidal dynamics from sea-level rise broadly match previous modelling studies of Pickering et al. (2012, 2017); however, there is uncertainty in simulating tidal changes due to sea-level rise—because of assumptions in coastline adjustment and tidal friction parameterisation in the model (i.e. no changes to tidal boundary conditions, no wetting and drying, and no morphodynamical changes were included). Nevertheless, we

Fig. 14 Mean difference in high water wave height between coupled and uncoupled models (δH_{sHW} as %), for January–February 2014 (**a**), and the relative change (as % of panel **a**) applying 0.44 m (**b**), 0.74 m (**c**) and 2.00 m (**d**) mean sea-level rise (MSLR) scenarios



have shown wave-tide interaction to be sensitive to changes in tidal dynamics—as sea-level rise-induced changes to tidal dynamics altered high water wave heights for all three scenarios throughout the computational domain (Fig. 11). Therefore, the tidal modulation of wave height may increase in the future due to sea-level rise-induced changes to tidal dynamics, which has implications globally, as the combined hazard of coastal flooding due to large waves at high tide may increase.

5 Conclusion

Dynamically coupled wave-tide modelling methods allow wave-tide interaction, and potential future changes to this process, to be investigated. The effect of tides in modulating nearshore wave height is investigated in the Irish Sea, with some regions experiencing a 20% increase in high water wave height due to tidal currents and elevation affecting the wave

field propagating into a coastal region. Such potential changes in the nearshore conditions will impact on flood hazard, and this uncertainty/error could propagate through to flood risk assessment. Therefore, wave-tide interaction has clear implications to the combined hazard of flooding from extreme sea-level and waves.

Simulated wave-tide interaction was shown to be sensitive to spatial model resolution because tidal currents are enhanced by bathymetric features requiring higher spatial resolution (e.g. an unstructured grid modelling approach) to simulate the current field accurately. Therefore, coupled models must therefore have rigorous validation strategies to ensure accuracy, and sub-kilometre-scale grid resolution appears necessary to capture tidal flow around bathymetric features (such as headlands). Moreover, wave-tide interaction appears sensitive

to potential future changes to tidal dynamics due to sea-level rise, with an increase in high water wave height. Future flood risk may increase in some regions as a result of the combined hazard of large waves occurring at times of high water—which has implications to flood risk mitigation strategy.

Funding This paper was the result of a collaboration funded by the Welsh Government and Higher Education Funding Council for Wales through the Sêr Cymru National Research Network for Low Carbon, Energy and Environment. SPN and MJL wish to acknowledge the support the Sêr Cymru National Research Network for Low Carbon, Energy and the Environment (NRN-LCEE) and the EPSRC METRIC project EP/R034664/1. MJL and PR wish to also acknowledge the support from the NERC funded ERIP project “CHEST” (NE/R009007/1). Finally, all authors wish to thank the organisers of the 15th Waves Workshop, hosted at Liverpool (UK), Bangor University MSc student Laura Ebeler and NERC Research Experience Placement student William Chang.

Appendix

Table 3 Comparison of wave validation statistics between the “medium” resolution (1/120°) coupled (COAWST) and uncoupled (SWAN) Irish Sea models

Buoy	Aberporth (Ab)		Met Erin (M)		Seacams (Sc)		Satellite track Hs validation	
Loc	52.37°N & 4.69°W		53.48°N & 5.43°W		53.22°N & 4.72°W		See Table 2	
Date period	03-Jan to 28-Feb 2014 (56 days)		1-Jan to 11-Jan 2014 (7 days)		03-Oct to 16-Nov 2014 (45 days)		See Table 2	
	SWAN	COWAST	SWAN	COWAST	SWAN	COWAST	SWAN	COWAST
Hs RMSE	0.66 m (10%)	0.64 m (9%)	0.64 m (16%)	0.65 m (16%)	0.35 m (7%)	0.41 m (8%)	0.50 m (34%)	0.51 m (36%)
RSQ	88%	90%	92%	92%	88%	79%	79%	78%
BIAS	28%	30%	44%	45%	−14%	3%	16%	17%
SI	27%	25%	29%	29%	19%	23%	24%	24%
Tz RMSE	0.9 s (14%)	1.1 s (16%)	—	—	0.7 s (16%)	0.9 s (19%)	—	—
RSQ	71%	72%	—	—	42%	37%	—	—
BIAS	13%	56%	—	—	−8%	15%	—	—
SI	16%	18%	—	—	14%	16%	—	—

Open Access This article is distributed under the terms of the Creative Commons Attribution 4.0 International License (<http://creativecommons.org/licenses/by/4.0/>), which permits unrestricted use, distribution, and reproduction in any medium, provided you give appropriate credit to the original author(s) and the source, provide a link to the Creative Commons license, and indicate if changes were made.

References

- Ardhuin F, Roland A, Dumas F, Bennis AC, Sentchev A, Forget P, Wolf J, Girard F, Osuna P, Benoit M (2012) Numerical wave modeling in conditions with strong currents: dissipation, refraction, and relative wind. *J Phys Oceanogr* 42(12):2101–2120
- Ardhuin F, Gille ST, Menemenlis D, Rocha CB, Rasche N, Chapron B, Gula J, Molesmaker J (2017) Small-scale open-ocean currents have large effects on wind-wave heights. *J Geophys Res Oceans*. <https://doi.org/10.1002/2016JC012413>
- Arns A, Dangendorf S, Jensen J, Talke S, Bender J, Pattiaratchi C (2017) Sea-level rise induced amplification of coastal protection design heights. *Sci Rep* 7:40171
- Booij N, Ris RC, Holthuijsen LH (1999) A third-generation wave model for coastal regions—I. Model description and validation. *J Geophys Res* 104:7649–7666
- Brown JM (2010) A comparison of WAM and SWAN under storm conditions in a shallow water application. *Ocean Model* 35(3):215–229
- Brown JM, Souza AJ, Wolf J (2010) An investigation of recent decadal-scale storm events in the eastern Irish Sea. *J Geophys Res* 115:1–12
- Brown JM, Bolanos R, Wolf J (2011) Impact assessment of advanced coupling features in a tide-surge-wave model, POLCOMS-WAM, in a shallow water application. *J Mar Syst* 87:13–24
- Bunya S, Dietrich JC, Westerink JJ, Ebersole BA, Smith JM, Atkinson JH, Jensen R, Resio DT, Luettich RA, Dawson C, Cardone VJ (2010) A high-resolution coupled riverine flow, tide, wind, wind wave, and storm surge model for southern Louisiana and Mississippi. Part I: model development and validation. *Mon Weather Rev* 138(2):345–377

- Carrere L, Lyard F, Cancet M, Guillot A, Roblou L (2012) FES2012: a new global tidal model taking advantage of nearly 20 years of altimetry. In: Proceedings of meeting 20 Years of Altimetry, Venice
- Dee DP, Uppala SM, Simmons AJ, Berrisford P, Poli P, Kobayashi S, Andrae U, Balmaseda MA, Balsamo G, Bauer DP, Bechtold P (2011) The ERA-Interim reanalysis: Configuration and performance of the data assimilation system. *Q J R Meteorol Soc* 137(656):553–597
- Dietrich JC, Zijlema M, Westerink JJ, Holthuijsen LH, Dawson C, Luettich RA Jr, Jensen RE, Smith JM, Stelling GS, Stone GW (2011) Modeling hurricane waves and storm surge using integral-coupled, scalable computations. *Coast Eng* 58(1):45–65
- Fan Y, Ginis I, Hara T, Wright CW, Walsh E (2009a) Numerical simulations and observations of surface wave fields under an extreme tropical cyclone. *J Phys Oceanogr* 39:2097–2116
- Fan Y, Ginis I, Hara T (2009b) The effect of wind-wave-current interaction on air-sea momentum fluxes and ocean response in tropical cyclones. *J Phys Oceanogr* 39:1019–1034
- Flato G, et al (2013) Evaluation of climate models. In: Climate change 2013: the physical science basis. WG I contribution to the Fifth Assessment Report of the Intergovernmental Panel on Climate Change
- Gallien TW, Sanders BF, Flick RE (2014) Urban coastal flood prediction: Integrating wave overtopping, flood defence and drainage. *Coast Eng* 91:18–28
- Haidvogel DB, Arango H, Budgell WP, Cornuelle BD, Curchitser E, Di Lorenzo E (2008) Ocean forecasting in terrain-following coordinates: formulation and skill assessment of the regional ocean modeling system. *J Comput Phys* 227(7):3595–624
- Hashemi MR, Neill SP, Davies AG (2015) A couple tide-wave model for the NW European shelf seas. *Geophys Astrophys Fluid Dyn* 109(3): 234–253
- Hashemi MR, Grilli ST, Neill SP (2016) A simplified method to estimate tidal current effects on the ocean wave power resource. *Renew Energy* 96:257–269
- Hemer MA, Katzfey J, Trenham CE (2013) Global dynamical projections of surface ocean wave climate for a future high greenhouse gas emission scenario. *Ocean Model* 70:221–245
- Holthuijsen LH, Tolman HL (1991) Effects of the Gulf Stream on ocean waves. *J Geophys Res* 96(C7):12771–12775
- Hope ME, Westerink JJ, Kennedy AB, Kerr PC, Dietrich JC, Dawson C, Bender CJ, Smith JM, Jensen RE, Zijlema M, Holthuijsen LH (2013) Hindcast and validation of Hurricane Ike (2008) waves, fore-runner, and storm surge. *J Geophys Res: Oceans* 118(9):4424–4460
- Horsburgh KJ, Wilson C (2007) Tide-surge interaction and its role in the distribution of surge residuals in the North Sea. *J Geophys Res* 112: C08003
- Huntingford C, Marsh T, Scaife AA, Kendon EJ, Hannaford J, Kay AL, Lockwood M, Prudhomme C, Reynard NS, Parry S, Lowe JA (2014) Potential influences on the United Kingdom's floods of winter 2013/14. *Nature Climate Change* 4(9):769
- IPCC (2013) Summary for policymakers. In: Stocker TF, Qin D, Plattner G-K, Tignor M, Allen SK, Boschung J, Nauels A, Xia Y, Bex V, Midgley PM (eds) Climate change 2013: the physical science basis. Contribution of Working Group I to the Fifth Assessment Report of the Intergovernmental Panel on Climate Change. Cambridge University Press, United Kingdom
- Kendon M, McCarthy M (2015) The UK's wet and stormy winter of 2013/2014. *Weather* 70(2):40–47
- Kumar N, Voulgaris G, Warner JC, Olabarrieta M (2012) Implementation of the vortex force formalisation in the coupled ocean-atmosphere-wave-sediment transport (COAWST) modeling system for inner shelf and surf zone applications. *Ocean Model* 47:65–95
- Leonard M, Westra S, Phatak A, Lambert M, van den Hurk B, McInnes K, Risbey J, Schuster S, Jakob D, Stafford-Smith M (2014) A compound event framework for understanding extreme impacts. *Wiley Interdiscip Rev Clim Chang* 5(1):113–128
- Lewis M, Horsburgh K, Bates P, Smith R (2011) Quantifying the uncertainty in future coastal flood risk estimates for the UK. *J Coast Res* 27(5):870–881
- Lewis M, Schumann G, Bates P, Horsburgh K (2013) Understanding the variability of an extreme storm tide along a coastline. *Estuar Coast Shelf Sci* 123:19–25
- Lewis MJ, Neill SP, Hashemi MR, Reza M (2014) Realistic wave conditions and their influence on quantifying the tidal stream energy resource. *Appl Energy* 136:495–508
- Lewis M, Neill SP, Robins PE, Hashemi MR (2015) Resource assessment for future generations of tidal-stream energy arrays. *Energy* 83:403–415
- Lewis M, Neill SP, Robins P, Hashemi MR, Ward S (2017) Characteristics of the velocity profile at tidal-stream energy sites. *Renew Energy* 114:258–272
- Lewis HW, Sanchez JMC, Graham J, Saulter A, Bornemann J, Arnold A, Fallmann J, Harris C, Pearson D, Ramsdale S, Martínez-de la Torre A (2018) The UKC2 regional coupled environmental prediction system. *Geosci Model Dev* 11(1):1
- Maskell J, Horsburgh K, Lewis M, Bates P (2013) Investigating river-surge interaction in idealised estuaries. *J Coast Res* 30(2):248–259
- McGranahan G, Balk D, Anderson B (2007) The rising tide: assessing the risks of climate change and human settlement in low elevation coastal zones. *Environ Urban* 19:17–37
- Muis S, Verlaan M, Winsemius HC, Aerts J, Ward P (2016) A global reanalysis of storm surges and extreme sea levels. *Nat Commun*. <https://doi.org/10.1038/ncomms11969>
- Neill SP, Hashemi MR (2013) Wave power variability over the northwest European shelf seas. *Appl Energy* 106:31–46
- Neill SP, Lewis MJ, Hashemi MR, Slater E, Lawrence J, Spall SA (2014) Inter-annual and inter-seasonal variability of the Orkney wave power resource. *Appl Energy* 132:339–348
- Neill SP, Angeloudis A, Robins PE, Walkington I, Ward SL, Masters I, Lewis MJ, Piano M, Avdis A, Piggott MD, Aggidis G (2018) Tidal range energy resource and optimization—Past perspectives and future challenges. *Renew Energy*. <https://doi.org/10.1016/j.renene.2018.05.007>
- Palmer T, Stratton T, Saulter A, Henley E (2015) Case study comparisons of UK macro-tidal regime wave and current interaction processes; mesoscale wave model versus coastal buoy data. In: Proceedings of the 14th International Workshop on Wave Hindcasting and Forecasting and 5th Coastal Hazard Symposium, Florida Keys, USA
- Phillips OM (1977) The dynamics of the upper ocean. Cambridge University Press, New York 336pp
- Phillips B, Brown J, Bidlot JR, Plater A (2017) Role of beach morphology in wave overtopping hazard assessment. *J Marine Sci Eng* 5(1). <https://doi.org/10.3390/jmse5010001>
- Pickering MD, Wells NC, Horsburgh KJ, Green JAM (2012) The impact of future sea-level rise on the European Shelf tides. *Cont Shelf Res* 35:1–15
- Pickering MD, Horsburgh KJ, Blundell JR, Hirschi JM, Nicholls RJ, Verlaan M, Wells NC (2017) The impact of future sea-level rise on the global tides. *Cont Shelf Res* 142:50–68
- Prime T, Brown JM, Plater AJ (2015) Physical and economic impacts of sea-level rise and low probability flooding events on coastal communities. *PLoS One* 10(2):e0117030. <https://doi.org/10.1371/journal.pone.0117030>
- Prime T, Brown J, Platter A (2016) Flood inundation uncertainty: the case of a 0.5% annual probability flood event. *Environ Sci Policy* 59:1–9
- Pugh DT (1996) Tides, surges and mean sea-levels: a handbook for engineers. John Wiley & Sons, Chichester 427p
- Pullen T, Allsop NWH, Bruce T, Kortenhaus A, Schüttrumpf H, Van der Meer JW (2007) EurOtop, European overtopping manual-wave

- overtopping of sea defences and related structures: assessment manual. Also published as special volume of *Die Küste*
- Rapizo H, Babanin AV, Provis D, Rogers WE (2017) Current-induced dissipation in spectral wave models. *J Geophys Res Oceans* 122: 2205–2225
- Rapizo H, Durrant TH, Babanin AV (2018) An assessment of the impact of surface currents on wave modelling in the Southern Ocean. *Ocean Dyn* 68:939–955
- Roland A, Zhang YJ, Wang HV, Meng Y, Teng Y, Maderich V, Brovchenko I, Dutour-Sikiric M, Zanke U (2012) A fully coupled 3D wave-current interaction model on unstructured grids. *J Geophys Res* 117:C11
- Shchepetkin AF, McWilliams JC (2005) Regional ocean model system: a split-explicit ocean model with a free-surface and topography-following vertical coordinate. *Ocean Model* 9:347–404
- Sibley A, Cox D, Tittley H (2015) Coastal flooding in England and Wales from Atlantic and North Sea storms during the 2013/2014 winter. *Weather* 70(2):62–70
- Souza AJ, Brown JM, Williams JJ, Lymbery G (2013) Application of an operational storm coastal impact forecasting system. *J Oper Oceanogr* 6(1):23–26
- Staneva J, Wahle K, Gunther H, Stanev E (2016) Coupling of wave and circulation models in coastal-ocean predicting systems: a case study for the German Bight. *Ocean Sci* 12:797–806
- Stockdon HF, Holman RA, Howd PA, Sallenger AH Jr (2006) Empirical parameterization of setup, swash, and runup. *Coast Eng* 53(7):573–588
- Van der Meer, Horst W, van Velzen C (2009) Calculation of fragility curves for flood defence assets. *Flood Risk Manag Res Pract* 567–573
- Warner JC, Sherwood CR, Signell RP, Harris CK, Arango HG (2008a) Development of a three dimensional, regional, coupled wave, current and sediment transport model. *Comput Geosci* 34:1284–1306
- Warner JC, Perlin N, Skillingstad ED (2008b) Using the model coupling toolkit to couple earth system model. *Environ Model Softw* 23: 1240–1249
- Warner JC, Armstrong B, He R, Zambon JB (2010) Development of a coupled ocean-atmosphere-wave-sediment transport (COAWST) modelling system. *Ocean Model* 35:230–244
- Weisse R, Bellaïfiore D, Menéndez M, Méndez F, Nicholls RJ, Umgiesser G, Willems P (2014) Changing extreme sea levels along European coasts. *Coast Eng* 87:4–14
- Westerink JJ, Luetich RA, Feyen JC, Atkinson JH, Dawson C, Roberts HJ, Powell MD, Dunion JP, Kubatko EJ, Pourtaheri H (2008) A basin-to channel-scale unstructured grid hurricane storm surge model applied to southern Louisiana. *Mon Weather Rev* 136(3):833–864
- Wolf J (2008) Coupled wave and surge modelling and implications for coastal flooding. *Adv Geosci* 17:1–4
- Wolf J (2009) Coastal flooding: impacts of coupled wave-surge-tide models. *Nat Hazards* 49:241–260
- Woodworth PL, Teferle FN, Bingley RM, Shennan I, Williams SDP (2009) Trends in U.K. mean sea level revisited. *Geophys J Int* 176:19–30